




Prediction of Vehicle Form Feature for Cross-model Evolution Based on Improved Nonlinear Grey Bernoulli Model

Qiu Ying Xu¹, Ju Chen² and He Min Yan³

¹Guangzhou Panyu Polytechnic, xuqiuying@126.com

²Guangzhou Panyu Polytechnic, chenju2011@gmail.com

³IAT Automobile Technology CO., Ltd, yanhemin@126.com

Corresponding author: Ju Chen, chenju2011@gmail.com

Abstract. This paper presents a novel approach dealing with quantitative cross-model evolution of vehicle form features. The proposed model relies on a combination of data-driven and algorithm methods. The Morphological-Homogenization Method is used to determine the relationship between the affected and influenced models along different evolutionary axes. Due to the poor samples size, irregularity, and high oscillatory of form feature changes across generations, a combination of nonlinear grey Bernoulli model and Genetic Algorithm is used. The nonlinear grey Bernoulli model is improved with system latency and time-varying parameters, and Genetic Algorithm is used to optimize the model parameters. The results show that the improved model is more accurate than the Nash nonlinear grey Bernoulli model and is efficient in handling nonlinear sequences. This study uses the contour line of a specific brand's headlamp as a design example. Multiple transformations are applied to the three-dimensional styling while ensuring that the predicted headlamp front view profile remains unchanged. The goal is to provide designers with various styling references and valuable recommendations for both mature and developing manufacturers.

Keywords: Brand identity; Vehicle form features; Nonlinear grey Bernoulli model; Genetic Algorithm; Cross-model evolution.

DOI: <https://doi.org/10.14733/cadaps.2023.1074-1093>

1 INTRODUCTION

Consistent form features of vehicles are crucial in maintaining and strengthening brand identity. Many manufacturers have their own distinctive and recognizable product appearance [20]. Vehicle design consists of a combination of feature elements such as fenders, grilles, headlights, and windows, which are either shaped similarly or related to previous designs [19]. Despite many automotive manufacturers (e.g., BMW) keeps innovating their vehicles' aesthetics, the consumers can easily and quickly recognize them from the competitors.

Global market competition and the diversification of customer demand have greatly shortened the vehicle development cycle. To remain competitive, enterprises must adopt low-cost and fast-response design methods and offer new products that maintain critical characteristics based on existing model forms. As a result, the evolution of vehicle form features has become one of the most challenging problems in the design field [43]. This research aims to provide valuable recommendations for the industry and guidelines for mature and developing manufacturers.

Several renowned companies such as B&O (Denmark), Alessi (Italy), and Samsung (South Korea) have established a well-developed theory on product evolution research. Additionally, automobile companies, including Mercedes-Benz, General Motors, Ford, and Audi, have been engaged in extensive research on the evolution of car appearance over an extended period of time. The challenges in developing car styling DNA have been discussed [1], and the inheritance and evolution of the Audi A6 styling genes have been analyzed [45]. Shahrman [27] proposed a new design method for product innovation and improvement by taking the general principles of heredity and variation in biology and applying them to car design. The evolution of form characteristics in cars is comparable to the inheritance and evolution of biological genes.

The primary objective of this research is to develop a novel approach for quantitatively predicting cross-model evolution, which is becoming increasingly common in the vehicle design process. The structure of the paper is as follows. Section 2 reviews relevant literature on the topic. Section 3 discusses the Cross-model evolution and the vehicle morphological method. Section 4 describes the basic concepts of the general Nonlinear grey Bernoulli model (NGBM(1,1)) and the improved model based on Genetic Algorithm (GA). This section also presents evidence demonstrating the superiority of the improved NGBM(1,1) over the optimized Nash NGBM(1,1) method proposed by Wang (2013a). Section 5 predicts the positions of vehicle form feature points using data acquisition and simulation. A detailed comparison between different models is carried out, which shows that the improved NGBM(1,1) outperforms others. Various 3D design schemes are explored according to some transformation rules based on the predicted result in the front view. Finally, the paper concludes with comments and future research directions in Section 6, followed by references.

2 LITERATURE REVIEW

The objective of this research is to introduce a data-driven and algorithm-based approach to predict the evolution of vehicle form features quantitatively. Conventional vehicle styling design methods often involve qualitative approaches, including subjective intuition and experience-based judgments by designers, as well as Kansei engineering [3] and cognitive psychology [20]. However, these methods have limitations such as subjectivity, randomness, and inconsistency [17]. By transforming vehicle form features into specific data, this study aims to perform quantitative analysis and prediction to provide more precise design information and enhance the objectivity of form prediction.

2.1 Data-driven Design Method

Integrating data-driven design methods into the vehicle styling process can significantly improve the efficiency and effectiveness of the design process. This study builds upon previous research, such as the work of Lin [21] who used data mining techniques to optimize creative ability, Amitash [2] who developed a tool to support the creation of novel ideas through data mining algorithms, and Pan [24] who introduced a data-driven methodology to identify regions of design visual attraction that impact aesthetic appeal in automobile styling. Toh [33] also investigated the role of data mining techniques in determining the creativity of design ideas. Deng [10] established quantitative criteria to assist mini-car manufacturers in improving brand recognition. Usama [34] proposed a data-driven design pipeline for quick exploration of design alternatives for vehicle performance and appearance. Yang [42] presented a data mining method for resolving the contradictions and conflicts associated with product brand recognition.

These works have been shown to improve the efficiency and effectiveness of the design process, as well as enhance the creativity and objectivity of the design outcome. The previous research studies have demonstrated the application of data mining techniques, data-driven methodologies, and quantitative criteria in vehicle styling design, and have provided valuable insights into the integration of data-driven strategy into the design process.

2.2 Algorithm-based Method

The utilization of algorithm-based methods has become increasingly popular in the realm of computational design exploration, particularly in regard to car styling. Shieh [28] combined the principles of Kansei engineering with evolutionary algorithms to generate designs for vases. Hyun [18] emphasized the importance of utilizing flexible computational methods, specifically those based on genetic algorithms, to explore forms and generate many concepts. Wang [36] and Jing [19] applied genetic algorithms to the problem of automobile design, demonstrating its effectiveness as a method. Su [30] presented a decision-making approach for generating and optimizing vehicle images using particle swarm optimization. Luo [22] and Ding [12] utilized genetic algorithms to develop technology for generating and optimizing car styling decisions.

Various studies have demonstrated these methods' effectiveness, including using genetic algorithms for form exploration and generating numerous concepts, algorithm-based methods have proven to be valuable tools for computational design exploration, particularly in the field of automobile styling.

The prediction of vehicle form feature evolution is often a challenge due to the small number of evolutionary generations in most cases. Deng [9] proposed a grey forecasting model, Grey Model (GM(1,1)), which uses four datasets to make predictions. This model has been applied in forecasting the new BMW styling [40] and vehicle form evolution [41]. However, traditional grey forecasting models are often too simple to achieve high precision, leading researchers to explore the use of hybrid grey models that combine multiple models for better predictions, such as Grey-Fuzzy [32], Grey-Markov [31], Grey-Artificial Neural Network [15,26], and Grey-Fourier [8,37]. The increasing complexity of these mathematical models has made them difficult to understand and widely apply. The nonlinear grey Bernoulli model [6, 25], also known as NGBM(1,1), is an effective grey forecasting model and a first-order one-variable grey Bernoulli differential equation. This model has a power exponent μ that can effectively reflect the nonlinear characteristics of real systems and provides a flexible approach to determining vehicle contours.

Additionally, the design of vehicles across generations frequently changes in unpredictable ways, making it challenging to interpret and analyze these changes. The series of data representing vehicle feature points' positions are often irregular, chaotic, and highly oscillate. The standard NGBM(1,1) model may not be suitable for handling this type of oscillating data, so researchers have introduced system latency and time-varying parameters into the model to create an improved version of the NGBM(1,1) model. The parameters of this improved model are optimized using GA, which significantly increases in the accuracy of the simulation of fluctuant data.

In conclusion, the use of GA in optimization problems has been well established, with a history dating back to Holland's introduction of the idea based on Darwin's theory of natural selection [14]. It has been widely applied in various fields, including optimizing internal parameters in grey forecasting models [4,16] and parameters in support vector regression for higher forecast accuracy [13]. GA has also been used in data mining [7] and evolutionary design methods, such as the spider-web inspired design method proposed by Zhang [44]. Overall, the versatility and effectiveness of GA in solving complex optimization problems make it a valuable tool in various fields of research and industry.

3 THE CROSS-MODEL EVOLUTION AND MORPHOLOGICAL-HOMOGENIZATION METHOD

3.1 The Cross-model Evolution

There are two ways for vehicle form feature evolution: the same-model and the cross-model. The former refers to the inheritance and reuse of form features among the same models, such as the repeated use of the front face feature in the series of Benz C-Class, as shown in Figure 1. The latter refers to the transfer of form features from one model to another, such as the shared form characteristics between the Q3, Q5, and Q7 of Audi, as seen in Figure 2. The "tiger roaring" front face design of Kia was first implemented in the K5 and later appeared in the K2, contributing to Kia's position as a leading Asian vehicle brand, as depicted in Figure 3. Both methods play a significant role in the evolution of vehicle form features, but the cross-model evolution has received more attention in recent years due to its ability to bring new design elements into a series while maintaining a sense of brand consistency.

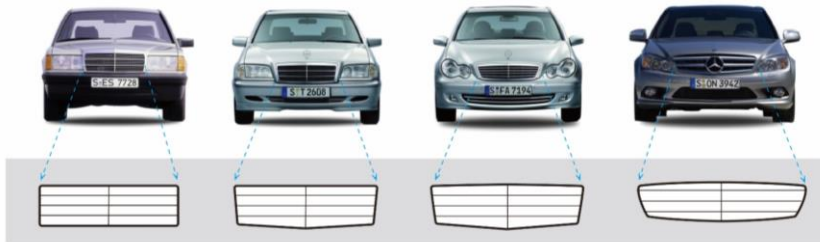


Figure 1: The consistent front face feature of Benz C-Class.

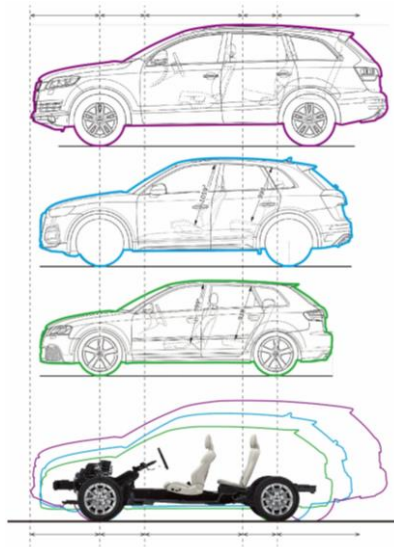


Figure 2: Q5 and Q7 of Audi share the mutual form characteristics.

Automakers often adopt parts-sharing strategies to reduce research and development costs and alleviate market competition. An example of this is the acquisition of Bentley by Volkswagen Group in 1998, where the Continental GT model and Volkswagen's Phaeton utilized the same chassis, engine, transmission system, and other components.



Figure 3: The "Tiger roaring" front face of Kia K2 and K5.

In the cross-model evolution, two axes of evolution are defined: the horizontal and vertical axes. The former refers to the main evolutionary process of a specific model, while the latter refers to the influence other models from different brands or categories have on the model on the horizontal axis. The models on the horizontal axis are referred to as "affected models", while those on the vertical axis are referred to as "influenced models". An example of this can be seen in the evolution of the Lexus GS series, where the LF-GH Concept model (2011) influenced the Lexus GS (2012-2015), which was the affected model, as shown in Figure 4. Similarly, in the evolution of Mercedes-Benz, the A-Concept model (2011) influenced the A-Class (2012-2018), which was the affected model, as shown in Figure 5.



Figure 4: The evolution process of Lexus GS series.

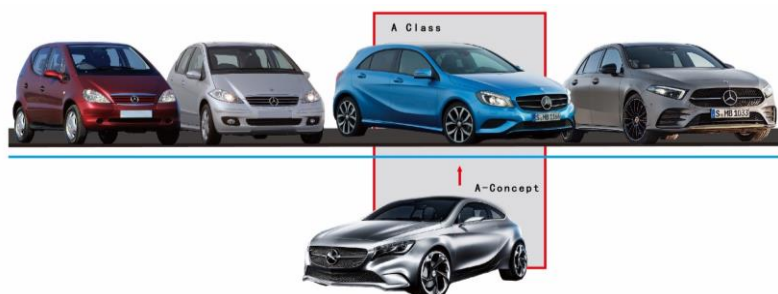


Figure 5: The evolution process of Benz A-Class.

3.2 The Morphological-Homogenization Method

The author has developed a form feature prediction model for same-model evolution called the IGMBPM model, which is effective for handling poor samples and highly oscillate data sequences. However, the prediction of cross-model evolution is more complex, and requires the use of the

Morphological-Homogenization Method (MHM) to address the quantification problem between affected and influenced models.

MHM takes various features, such as points, lines, or surfaces, and calculates a representative shape by averaging or assigning different weights to a set of shapes. The result is then quantified and used to predict new forms. For example, bottles B and D can be averaged to obtain bottle C, which can be considered as an interpolation of bottles B and D. Bottles A and E can be added with weights of 3:1 and 1:3, respectively, to obtain new forms that can be used as the extrapolation results of bottles B and D. This process is illustrated in Figure 6.

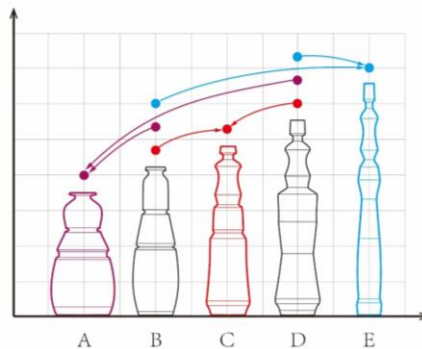


Figure 6: The Morphological-Homogenization Method.

When the evolution way of a vehicle's form feature is cross-model, the position of each vehicle form feature point on the horizontal axis is expressed as $p_{ij} = (x_{ij}, y_{ij})$, the original sequence of positions is $X_i = \{x_{i1}, x_{i2}, \dots, x_{mk}\}$, $Y_i = \{y_{i1}, y_{i2}, \dots, y_{mk}\}$, where $i = 1, 2, 3, \dots, m$, $j = 1, 2, 3, \dots, k$, m is the number of form feature points, k is the number of vehicle evolutionary generations on the horizontal axis.

While the influenced vehicle form feature point coordinates on the vertical axis are marked as $p_{i0} = (x_{i0}, y_{i0})$, d is the weight of the affected model and the influenced model, $p_{ij} = (x_{ij}, y_{ij})$ will be replaced by $p'_{ij} = (x'_{ij}, y'_{ij})$.

$$\begin{aligned} x'_{ij} &= x_{ij} \times d + x_{i0} \times (1 - d), \\ y'_{ij} &= y_{ij} \times d + y_{i0} \times (1 - d). \end{aligned} \quad (1)$$

4 METHODS

4.1 The General NGBM(1,1)

NGBM(1,1) is an essential extension of the traditional GM(1,1) combined with the Bernoulli differential equations. Comparatively, the NGBM(1,1) model performs better than the GM(1,1) model in having an exponential value u that fits the actual data well. Thus, the model can realistically reflect the feature of non-linearity in data as evidenced by high simulation and forecasting accuracy. The model includes the following steps:

Step 1: Let an original series

$$X^{(0)} = (x^{(0)}(1), x^{(0)}(2), \dots, x^{(0)}(m)). \quad (2)$$

In this equation $x^{(0)}(k)$ is the value of the behavior series at k , $k = 1, 2, 3, \dots, m$.

Step 2: The 1-AGO (the first-order accumulating generator operator) series of $X^{(0)}$ can be obtained by imposing the first order accumulating generator operator:

$$X^{(1)} = (x^{(1)}(1), x^{(1)}(2), \dots, x^{(1)}(m)), \text{ where } x^{(1)}(k) = \sum_{i=1}^k x^{(0)}(i). \quad (3)$$

Step 3: The grey differential equation of the NGBM(1,1) model is:

$$x^{(0)}(k) + az^{(1)}(k) = b(z^{(1)}(k))^\mu, k = 2, 3, \dots, m, \quad (4)$$

Where $x^{(0)}(k)$ is called a grey derivative, and $z^{(1)}(k) = 0.5x^{(1)}(k) + 0.5x^{(1)}(k - 1)$ is referred to as the background value of the grey derivative.

When $\mu = 0$, the NGBM(1,1) model is equal to the traditional GM(1,1) model; when $\mu = 2$, the NGBM(1,1) model is equal to the grey Verhulst model.

Step 4: Least Squares Estimation of a and b according to Eq. (4):

$$(a, b)^T = (B^T B)^{-1} B^T Y, \tag{5}$$

$$\text{Where } B = \begin{bmatrix} -z^{(1)}(2) & (z^{(1)}(2))^\mu \\ -z^{(1)}(3) & (z^{(1)}(3))^\mu \\ \vdots & \vdots \\ -z^{(1)}(m) & (z^{(1)}(m))^\mu \end{bmatrix}, \quad Y = \begin{bmatrix} x^{(0)}(2) \\ x^{(0)}(3) \\ \vdots \\ x^{(0)}(m) \end{bmatrix}. \tag{6}$$

Step 5: The whitenization differential equation of the NGBM(1,1) model, a first differential equation, can be established based on $X^{(1)}$:

$$\frac{dx^{(1)}(k)}{dt} + ax^{(1)}(k) = b(x^{(1)}(k))^\mu, \tag{7}$$

where a is the development coefficient, b is the grey actor, $\mu \neq 1$.

Step 6: Set initial value, $\hat{x}^{(1)}(1) = x^{(0)}(1)$, Eq. (7) can be solved as:

$$\hat{x}^{(1)}(k + 1) = \left\{ \frac{b}{a} + \left[x^{(0)}(1)^{1-\mu} - \frac{b}{a} \right] e^{-(1-\mu)ak} \right\}^{\frac{1}{1-\mu}}. \tag{8}$$

Step 7: Finally make first order inverse accumulated operation (1-IAGO) to $\hat{x}^{(1)}(k)$, and obtain simulation and forecasted value:

$$\hat{x}^{(0)} = \hat{x}^{(1)}(k) - \hat{x}^{(1)}(k - 1), k = 2, 3, \dots, m. \tag{9}$$

4.2 The Modeling Procedure of the Improved NGBM(1,1)

Wang [39] has demonstrated that the general NGBM(1,1) is more suitable for single-peak data rather than oscillating data, hence in this study, the general NGBM(1,1) is improved by GA.

Supposed $X^{(0)}$, $X^{(1)}$ and $Z^{(0)}$ is the original sequence, the 1-AGO sequence and the background value sequence respectively.

Step 1: The grey differential equation of the improved NGBM(1,1) model is:

$$x^{(0)}(k) + a \tan p(k - r) z^{(1)}(k - r) = b \sin p(k - r) (z^{(1)}(k - r))^\mu, \tag{10}$$

where $-a \tan p(k - r)$ is the development coefficient, $b \sin p(k - r)$ is the grey actor, r is system latency parameter, p is time-varying parameter, μ is power index, $\mu \neq 1$.

Step 2: Least Squares Estimation of a and b according to Eq.(4):

$$(a, b)^T = (B^T B)^{-1} B^T Y, \tag{11}$$

$$\text{where } (B^T B)^{-1} = \frac{1}{FG - C^2} \begin{bmatrix} G & C \\ C & F \end{bmatrix}, B^T Y = [-E \quad D]^T, \tag{12}$$

$$\text{where } C = \sum_{k=r+2}^m \sin p(k - r) \tan p(k - r) (z^{(1)}(k - r))^{\mu+1}, \tag{13}$$

$$F = \sum_{k=r+1}^m [\tan p(k - r) z^{(1)}(k - r)]^2, \tag{14}$$

$$G = \sum_{k=r+2}^m [\sin p(k - r) (z^{(1)}(k - r))^\mu]^2, \tag{15}$$

$$D = \sum_{k=r+2}^m \sin p(k - r) x^{(0)}(k) (z^{(1)}(k - r))^\mu, \tag{16}$$

$$E = \sum_{k=r+2}^m \tan p(k - r) x^{(0)}(k) z^{(1)}(k - r). \tag{17}$$

Step 3: The simulation and forecasted value is:

$$\hat{x}^{(0)}(k) = b \sin p(k-r)(0.5x^{(1)}(k-r) + 0.5x^{(1)}(k-r-1)^\mu - a \tan p(k-r)(0.5x^{(1)}(k-r) + 0.5x^{(1)}(k-r-1)) \tag{18}$$

4.3 The Parameters Optimization in the Improved NGBM(1,1) based on GA

In this study, we take advantage of the ability of the GA to solve optimization problems. As long as an appropriate fitness function is provided, the algorithm may generate a search direction that approximates the best value. This study uses GA is used to estimate the optimal parameters p and μ of the improved NGBM(1,1).

The estimation of parameters is a nonlinear programming problem, which can be defined as follows:

$$\min \text{MAPE} = \frac{1}{m-r-1} \sum_{k=2+r}^m \frac{|\hat{x}^{(0)}(k) - x^{(0)}(k)|}{x^{(0)}(k)}, \text{ s.t. } r \neq 1$$

$$\hat{x}^{(0)}(k) = b \sin p(k-r)(0.5x^{(1)}(k-r) + 0.5x^{(1)}(k-r-1)^\mu - a \tan p(k-r)(0.5x^{(1)}(k-r) + 0.5x^{(1)}(k-r-1)), k = 2+r, 3+r, \dots, m, \tag{19}$$

where MAPE is mean absolute percentage error.

GA is designed from starting with three genetic operators of selection, crossover and mutation. The steps of solving the optimization problem using the GA can be described as follows:

Step 1: Choose p and μ as the parameters to be optimized.

Step 2: Encode the parameters and randomly generate the parameters to form an initial population.

Step 3: Set Eq. (19) as the subjection function to calculate fitness value for each individual in the population.

Step 4: Perform the crossover operation between the two parent genomes in the population.

Step 5: Generate an offspring's genome by mutation.

Step 6: Go back to step 3, step 4 and step 5, after repeated iterations, until the optimal individual goals achieve to $0.001 \leq \varepsilon \leq 0.01$ and $\text{MAPE} \leq 0.01$, then stop the operation.

$$\varepsilon = \frac{|\hat{x}^{(0)}(k) - x^{(0)}(k)|}{x^{(0)}(k)} \tag{20}$$

Parameters	Value	Parameters	Value
Population Size	50	Mutation probability	0.01
The maximum number of genetic generations	100	The initial value of ε	1
Individual length	18	The initial value of MAPE	1
Crossover probability	0.5	The initial value of number of iterations	1

Table 1: The parameters of GA.

The parameters of GA are shown in Table 1.

Through the above process, we can use a GA to find the optimized p_{best} and μ_{best} , according to which a_{best} and b_{best} are obtained. Hence the optimized simulation value is:

$$\hat{x}^{(0)}(k) = b_{best} \sin p_{best}(k-r)(0.5x^{(1)}(k-r) + 0.5x^{(1)}(k-r-1)^{\mu_{best}} - a_{best} \tan p_{best}(k-r)(0.5x^{(1)}(k-r) + 0.5x^{(1)}(k-r-1)) \tag{21}$$

The flowchart of the improved NGBM(1,1) based on GA is illustrated in Figure 7. System latency parameter r and time-varying parameters p are introduced into the general NBGM(1,1), which

make the improved model more adaptive to small sample oscillating sequence than the general model.

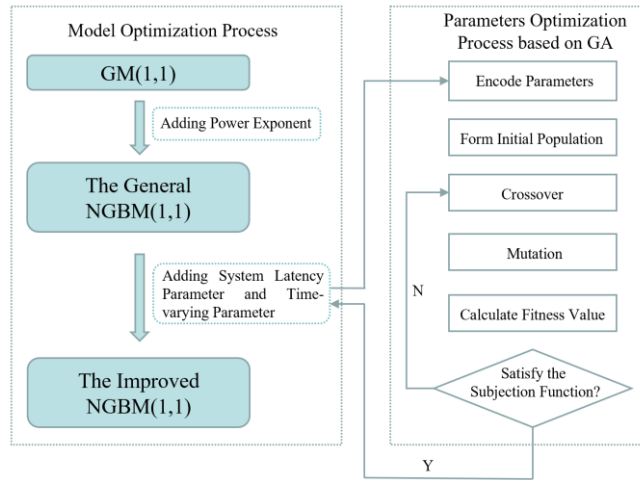


Figure 7: The flowchart of the improved NGBM(1,1) based on GA.

4.4 Evaluation of the Performance

The *ARPE* measures are the most commonly used accuracy measures in forecasting studies. Therefore, average relative percentage error (ARPE) is selected to evaluate the performance of models. The ARPE defined as follows:

$$ARPE = \frac{1}{k-1} \sum_{i=2}^k \left| \frac{x_i - \hat{x}_i}{x_i} \right| \times 100\% , i = 2,3,\dots,k. \tag{22}$$

Where x_i is the measured value, \hat{x}_i is the forecasted value, k is the generation number of vehicle form changing and upgrading.

The lower the *ARPE* value, the higher accuracy of the model. Delurgio [11] summarized the criteria of *ARPE* for model evaluation as shown in Table 2.

<i>ARPE</i> (%)	Forecasting Power
<10	Highly accurate
10-20	Good
20-50	Reasonable
>50	Inaccurate

Table 2: The Criteria of ARPE.

4.5 Verification of the Improved NGBM(1,1)

The improved Nash NGBM(1,1) model is demonstrated to be effective through a comparison of its accuracy with the general NGBM(1,1) model, using the export economic index for Chinese high technology enterprises as a case study. Wang [38] applied the optimized Nash NGBM(1,1) to simulate the value of the export index and achieved an ARPE of 9.12%. In the current study, the improved NGBM(1,1) model is also applied to the same data set and the results are shown in Table

2. The average simulation inaccuracy is decreased from 9.12% to 7.03%, proving the superiority of the improved Nash NGBM(1,1) over the general NGBM(1,1). This result confirms the effectiveness of the improved NGBM(1,1) model.

<i>Actual value (USD 100 million)</i>	<i>The optimized Nash NGBM(1,1) Simulated value</i>	<i>The improved NGBM(1,1) $r = 1, \mu = 1.6994, p = 1.9140$ Simulated value</i>
2646	2646	2646
3684	3684.00	3684.00
3564	3168.52	3448.41
2493	3161.98	2827.80
3595	3318.63	3435.44
<i>ARPE(%)</i>	9.12	7.03

Table 3: The comparison of simulated results.

5 RESULTS AND DISCUSSION

The purpose of this study is to investigate the cross-model evolution of vehicle form features using the improved forecasting model. The workflow consists of several parts, as illustrated in figure 8. The biggest challenge in the data acquisition process is how to convert morphological features into data. The improved forecasting model is applied to simulate the data, and the prediction results are then discussed. Finally, various design schemes are obtained based on transformation rules that can be useful for designers.

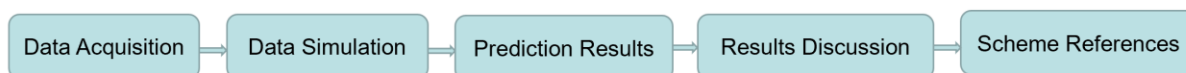


Figure 8: The workflow of vehicle form features prediction.

For example, the study focuses on a specific brand of vehicle, which has undergone nine generations of styling changes over nearly forty years.

Due to its economical, affordable, durable, and practical features, this brand is widely popular globally. With the advancement of design globalization, differentiation in design is giving way to convergence. The familial genetic traits have been spread across the entire product family, and the design elements of luxury models have started appearing on medium- and low-priced models.

The 9th generation was launched in 2014 and its front face was inspired by a luxury model from the same brand, giving the body a sense of high-tech and dynamism. As a result, this luxury model is regarded as the influenced model on the vertical evolutionary axis and had an impact on the 9th generation on the horizontal evolutionary axis. Figure 9 illustrates the evolutionary process of the headlamp.

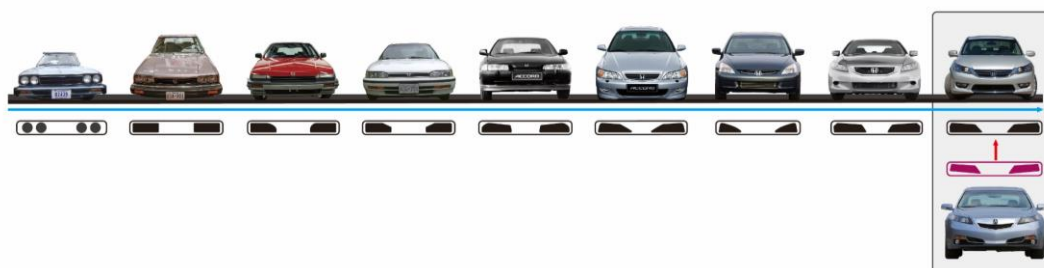


Figure 9: The headlamp evolutionary process.

5.1 The Original Sequence

Standardize the size of all vehicle models using a uniform front axle track measurement, and extract the headlamp profile using Alias AutoStudio software.

The headlamp is decomposed into four main lines (M_1, M_2, M_3, M_4) and four R-angle lines (R_1, R_2, R_3, R_4), as shown in figure 10(a). They are respectively described by NURBS third-order lines and 25 feature points will be obtained, as shown in figure 10(b). When the R-angle lines converge at one point, the headlamp has a sharp corner transition in its shape.

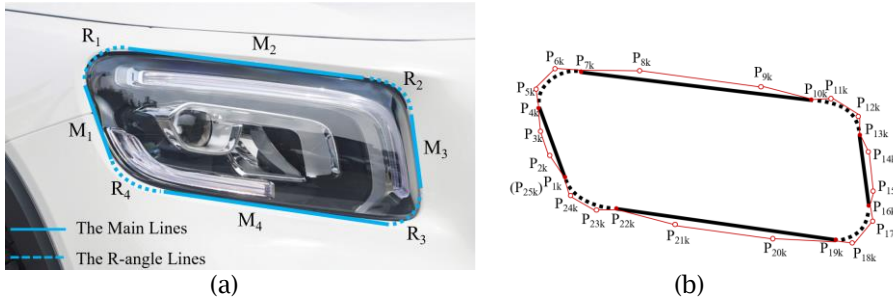


Figure 10: the composition of the headlamp contour.

The point of intersection vehicle front wheel center is the intersection point of axis X and axis Y in front view. The two-dimensional coordinates of each point is expressed as $p_{ij} = (x_{ij}, y_{ij})$. The original sequence of generational vehicle form feature points' position is:

$X_i = \{x_{i,1}, x_{i,2}, \dots, x_{i,25,9}, x_{i,25,TLM}\}, Y_i = \{y_{i,1}, y_{i,2}, \dots, y_{i,25,9}, y_{i,25,TLM}\}$, Where $i = 1, 2, 3, \dots, m$, $j = 1, 2, 3, \dots, k$, m is the number of form feature points, k is the number of vehicle evolutionary generations including the luxury model (abbreviated as TLM). $x_{i,1}$ to $x_{i,9}$ and $y_{i,1}$ to $y_{i,9}$ mean the X and Y coordinate of the first to the 9th generation, $x_{i,TLM}$ and $y_{i,TLM}$ mean the X and Y coordinate of the luxury model. Based on the MHM, the weight of the affected model (the 9th generation) on the horizontal axis and the influenced model (the luxury model) on the vertical axis is set as 3:1. $x'_{i,9} = 0.75x_{i,9} + 0.25x_{i,TLM}$, $y'_{i,9} = 0.75y_{i,9} + 0.25y_{i,TLM}$, $x_{i,9}$ will be replaced by $x'_{i,9}$, $y_{i,9}$ will be replaced by $y'_{i,9}$. $X'_i = \{x_{i,1}, x_{i,2}, \dots, x'_{i,25,9}\}$, $Y'_i = \{y_{i,1}, y_{i,2}, \dots, y'_{i,25,9}\}$, which is the new original sequence of improved NGBM(1,1), the new data sequence are shown in Appendix A.

5.2 The Prediction Proceed

Take X_{10} as example randomly, which is the point' position changing from the first to the 9th generation, $X_{10} = 46.59, 84.66, 138.67, 134.59, 94.75, 101.72, 86.19, 72.78, 52.11$. Based on the improved NGBM(1,1) with different system latency parameters, the simulated results and APRE are showed in Table 3.

Original data of X_{10}	Simulated results of Improved NGBM (1,1)						
	$r = 1$	$r = 2$	$r = 3$	$r = 4$	$r = 5$	$r = 6$	$r = 7$
46.59	46.59	46.59	46.59	46.59	46.59	46.59	46.59
84.66	84.66	84.66	84.66	84.66	84.66	84.66	84.66
138.67	138.67	138.67	138.67	138.67	138.67	138.67	138.67
134.59	125.31	129.07	134.59	134.59	134.59	134.59	134.59

94.75	109.66	115.68	121.64	94.75	94.75	94.75	94.75
101.72	98.34	98.92	106.52	117.02	101.72	101.72	101.72
86.19	86.26	85.59	87.12	91.57	111.30	86.19	86.19
72.78	69.96	71.10	70.41	69.10	72.78	54.80	72.78
52.11	53.08	52.11	52.11	52.11	51.13	160.12	97.26
ARPE%	3.53	3.55	4.16	2.93	3.44	2.58	9.63

Table 3: The original data and simulated results.

when $r = 1$, $p_{best} = 1.3525$, $\mu_{best} = -0.5282$, the value of ARPE is 3.53%, as shown in Figure 11(a); when $r = 2$, $p_{best} = -1.3171$, $\mu_{best} = -0.5236$, the value of ARPE is 3.55%, as shown in Figure 11(b); when $r = 3$, $p_{best} = 0.0928$, $\mu_{best} = -0.5305$, the value of ARPE is 4.16%, as shown in Figure 11(c); when $r = 4$, $p_{best} = 1.3230$, $\mu_{best} = -0.6777$, the value of ARPE is 2.93%, as shown in Figure 11(d); when $r = 5$, $p_{best} = 1.9122$, $\mu_{best} = -0.9451$, the value of ARPE is 3.44%, as shown in Figure 11(e); when $r = 6$, $p_{best} = 0.8504$, $\mu_{best} = 0.7571$, the value of ARPE is 2.58%, as shown in Figure 11(f); when $r = 7$, $p_{best} = 0.4174$, $\mu_{best} = 0.3958$, the value of ARPE is 9.63%, as shown in Figure 11(g).

When $r = 6$, the improved NGBM(1,1) get the minimal ARPE. Meanwhile, the improved NGBM(1,1) has remarkable decreased the model error than the general NGBM(1,1), no matter what system latency parameters is, the forecasting result of $x_{10,10}$ is 361.71.

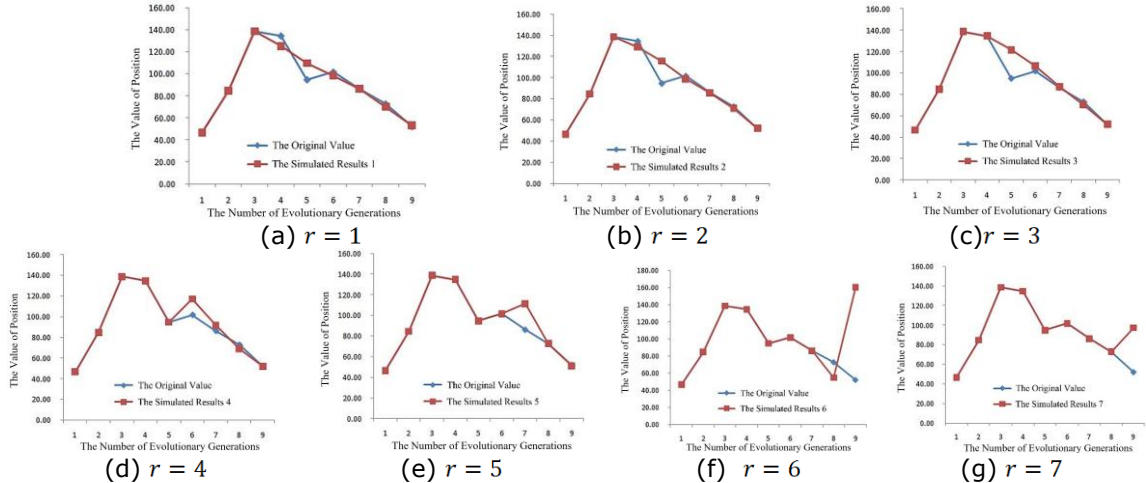


Figure 11: The comparison chart of the simulated results and the original data under different parameters.

5.3 The Prediction Results

Table 4 shows the prediction results of 25 feature points' coordinates of the tenth generation headlamp using the improved NGBM(1,1). Input the predicted results into Alias AutoStudio

software to obtain the headlamp contour line of the tenth generation in front view, as shown in Figure 12.

<i>Point' SN</i>	<i>Coordinates</i>	<i>Point' SN</i>	<i>Coordinates</i>	<i>Point' SN</i>	<i>Coordinates</i>
1	-29.37, 243.52	10	25.27, 275.57	19	138.55, 209.60
2	-31.58, 263.79	11	59.04, 268.29	20	69.45, 217.98
3	-28.33, 297.06	12	94.33, 260.34	21	-3.52, 227.57
4	-20.19, 298.27	13	120.36, 253.79	22	-29.37, 243.52
5	-19.36, 291.43	14	128.97, 246.20	23	-29.37, 243.52
6	6.56, 284.52	15	136.44, 229.09	24	-29.37, 243.52
7	19.81, 282.01	16	138.55, 209.60	25	-29.37, 243.52
8	21.03, 280.66	17	138.55, 209.60		
9	22.95, 278.45	18	138.55, 209.60		

Table 4: The prediction results of 25 feature points' coordinates of the tenth-generation headlamp.



Figure 12: The headlamp contour line of the tenth generation.

5.4 The Results Analysis

Various design schemes can be explored in three-dimensional space for the headlamp while ensuring that the front contour line remains unchanged. Figure 13 shows the initial 3D scheme, which has the same front contour as in Figure 12. The research listed 13 possible transformation rules, however they are not all. These schemes provide designers with different references.

The research presented 13 possible transformation rules, but this list is not exhaustive. These rules were grouped into four categories based on the number of main lines adjusted: one main line, two main lines, three main lines, and all main lines. When a main line is adjusted, the neighboring R-angle lines are also adjusted simultaneously. Although the adjustments made were slight and the limitations of the software display may not show significant distinctions, for enterprise automotive designers, even slight adjustments can open up numerous design possibilities.

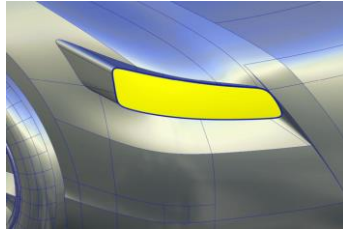


Figure 13: The initial 3D scheme of headlamp.

Transformation Rules 1: One main line is adjusted, two R-angle lines are linked				
Adjusted Lines	M ₁ is adjusted, R ₄ and R ₁ are linked	M ₂ is adjusted, R ₁ and R ₂ are linked	M ₃ is adjusted, R ₂ and R ₃ are linked	M ₄ is adjusted, R ₃ and R ₄ are linked
Front View Simplified Diagram				
3D Schemes				
Transformation Rules 2: Two main line are adjusted, three R-angle lines are linked				
Adjusted Lines	M ₁ and M ₂ are adjusted, R ₄ , R ₁ and R ₂ are linked	M ₂ and M ₃ are adjusted, R ₁ , R ₂ and R ₃ are linked	M ₃ and M ₄ are adjusted, R ₂ , R ₃ and R ₄ are linked	M ₄ and M ₁ are adjusted, R ₃ , R ₄ and R ₁ are linked
Front View Simplified Diagram				
3D Schemes				
Transformation Rules 3: Three main line are adjusted, four R-angle lines are linked				
Adjusted Lines	M ₁ , M ₂ and M ₃ are adjusted	M ₂ , M ₃ and M ₄ are adjusted	M ₃ , M ₄ and M ₁ are adjusted	M ₄ , M ₁ and M ₂ are adjusted
Front View Simplified Diagram				
3D Schemes				
Transformation Rules 4: Four main line are adjusted, four R-angle lines are linked				

Adjusted Lines	M_1, M_2, M_3 and M_4 are adjusted
Front View Simplified Diagram	
3D Schemes	

Table 5: the transformation rules and 3D schemes.

6 CONCLUSION AND THE FUTURE RESEARCH

This study focuses on a data-driven and algorithm-based method for the evolution of vehicle form features, with particular emphasis on cross-model evolution. The Morphological Homogenization Method is used to handle the relationship between the affected model and the influenced model. Changing the parameter d which determines the weight of the affected and influenced models can result in different forecasting results for the designers. The parameter can be adjusted according to the designer's understanding. However, in the actual conceptual design process, the influence from the vertical evolutionary axis will be more complex than the horizontal axis. There are not only luxury models of the same brand but also concept models or different models of the same brand that designers need to consider simultaneously. Therefore, quantifying various influences synthetically rather than separately is one of the future research focuses.

The transformation rules presented in subsection 5.4 are not exhaustive as they focus on the transformation of entire lines rather than individual points within a line. More complex transformations can arise from changes in the position of a single point within a line.

Furthermore, the data processing and forecasting procedures in this research may be challenging for vehicle designers without relevant knowledge background to understand and practice. Therefore, packaging the entire forecasting process into an overall service package is another challenge for the research team.

ACKNOWLEDGEMENT

This work was supported by the Ministry of education of Humanities and Social Science project under Research Grant (No: 22YJA760009), and the National Natural Science Foundation of China under Grant (Nos: 51663001, 52063002, 42061067), and Guangdong Provincial Philosophy and Social Science (No: 210223002), and School-level major social science projects (No: 21022428302). The funder had no role in study design, data collection and analysis, decision to publish, or preparation of the manuscript.

Qiuying Xu, <https://orcid.org/0000-0002-8781-1898>

Ju Chen, <https://orcid.org/0000-0002-8462-7278>

Hemin Yan, <https://orcid.org/0000-0003-0406-7002>

REFERENCES

- [1] Abidin, S. Z.; Othman; A.; Shamsuddin, Z.; Samsudin, Z.; Hassan, H.; Mohamed, W. A. W.: Identifying sequence maps or locus to represent the genetic structure or genome standard of

- styling DNA in automotive design, In *Advances on Mechanics, Design Engineering and Manufacturing*, 2017, 1159-1166. https://doi.org/10.1007/978-3-319-45781-9_116
- [2] Amitash O.; Lee H. K.; Lee M.: I-get: A Creativity Assistance Tool to Generate Perceptual Pictorial Metaphors. In *Proceedings of the 3rd International Conference on Human-Agent Interaction*. Association for Computing Machinery, 2015, 311-314. <https://doi.org/10.1145/2814940.2815006>
- [3] Cao, H.; Chen, Y.: A Kansei Engineering Based Method for Automobile Family Design, *International Conference on Applied Human Factors and Ergonomics*, Springer, Cham, 2018, 289-300. https://doi.org/10.1007/978-3-319-94944-4_32
- [4] Cayir Ervural, B.; Ervural, B.: Improvement of grey prediction models and their usage for energy demand forecasting, *Journal of Intelligent & Fuzzy Systems*, 34(4), 2018, 2679-2688. <https://doi.org/10.3233/jifs-17794>
- [5] Chen, H. Y.: The Research on the Relationship between Car Outline Form Imagery and the Distinguishing Features, Master thesis., National Cheng Kung University, Taiwan, 2001.
- [6] Chen, C. I.; Chen, H. L.; & Chen, S. P.: Forecasting of foreign exchange rates of Taiwan's major trading partners by novel nonlinear Grey Bernoulli model NGBM (1, 1), *Communications in Nonlinear Science and Numerical Simulation*, 13(6), 2008, 1194-1204. <https://doi.org/10.1016/j.cnsns.2006.08.008>
- [7] Chen, W.; Panahi, M.; Pourghasemi, H. R.: Performance evaluation of GIS-based new ensemble data mining techniques of adaptive neuro-fuzzy inference system (ANFIS) with genetic algorithm (GA), differential evolution (DE), and particle swarm optimization (PSO) for landslide spatial modelling. *Catena*, 157, 310-324, 2017. <https://doi.org/10.1016/j.catena.2017.05.034>
- [8] Dejamkhooy, A.; Dastfan, A.; Ahmadyfard, A.: Modeling and forecasting nonstationary voltage fluctuation based on grey system theory, *IEEE Transactions on Power Delivery*, 32(3), 2014, 1212-1219. <https://doi.org/10.1109/TPWRD.2014.2386696>
- [9] Deng, J. L.: *The elements on grey theory*, HUST Press, WuHan, WH, 2002.
- [10] Deng, W.; Kang, X.; Zhang, C.: Optimal Design of the Front Face of Minicars Based on Analytic Hierarchy Process, In *International Conference on Human-Computer Interaction*, 2017, 543-549.
- [11] DeLurgio, S. A.: *Forecasting principles and applications*, McGraw-Hill/Irwin, 1998.
- [12] Ding, M.; Bai, Z.: Product color emotional design adaptive to product shape feature variation, *Color Research & Application*, 44(5), 2017, 811-823. <https://doi.org/10.1002/col.22402>
- [13] Filgueiras, P. R.; Portela, N. A.; Silva, S. R.; Castro, E. V.; Oliveira, L. M.; Dias, J. C.; ... & Poppi, R. J.: Determination of saturates, aromatics, and polars in crude oil by ¹³C NMR and support vector regression with variable selection by genetic algorithm, *Energy & Fuels*, 30(3), 2016, 1972-1978. <https://doi.org/10.1021/acs.energyfuels.5b02377>
- [14] Holland, J. H.: *Adaptation in natural and artificial systems: an introductory analysis with applications to biology, control, and artificial intelligence*, MIT press, Cambridge, 1992.
- [15] Hao, H.; Zhang, Q.; Wang, Z.; Zhang, J.L.: Forecasting the number of end-of-life vehicles using a hybrid model based on grey model and artificial neural network, *Journal of cleaner production*, 202, 2018, 684-696. <https://doi.org/10.1016/j.jclepro.2018.08.176>
- [16] Hsu, L. C.: A genetic algorithm based nonlinear grey Bernoulli model for output forecasting in integrated circuit industry, *Expert systems with Applications*, 37(6), 2010, 4318-4323. <https://doi.org/10.1016/j.eswa.2009.11.068>
- [17] Hyun, K. H.; Lee, J.-H.; Kim, M.; Cho, S.: Style synthesis and analysis of car designs for style quantification based on product appearance similarities, *Advanced Engineering Informatics*, 29(3), 2015, 483-494. <https://doi.org/10.1016/j.aei.2015.04.001>
- [18] Hyun, K. H.; Lee, J. H.: Balancing homogeneity and heterogeneity in design exploration by synthesizing novel design alternatives based on genetic algorithm and strategic styling decision, *Advanced Engineering Informatics*, 38, 2018, 113-128. <https://doi.org/10.1016/j.aei.2018.06.005>

- [19] Jing, Z. C.; Zhao, J. H.: Optimization Design Method of Automobile Styling Based on Evolution Strategy, *China Mechanical Engineering*, 25(11), 2014, 1517-1523. <https://doi.org/10.3969/j.issn.1004-132X.2014.11.018>
- [20] Karjalainen, T. M.; Snelders, D.: Designing visual recognition for the brand, *Journal of Product Innovation Management*, 27(1), 2009, 6-22. <https://doi.org/10.1111/j.1540-5885.2009.00696.x>
- [21] Lin, C. F.; Yeh, Y. C.; Hung, Y. H.; Chang R., I.: Data mining for providing a personalized learning path in creativity: An application of decision trees, *Computers & Education*, 68, 2013.199-210. <https://doi.org/10.1016/j.compedu.2013.05.009>.
- [22] Luo, S. J., Li, W. J.; Fu, Y. T.: Consumer Preference-driven SUV Product Family Profile Gene Design, *Journal of Mechanical Engineering*, 25(2), 2016, 173-181. <https://doi.org/10.3901/JME.2016.02.173>
- [23] Ostrosi, E.; Bluntzer, J. B.; Zhang, Z.; Stjepandić, J.: Car style-holon recognition in computer-aided design, *Journal of computational design and engineering*, 6(4), 2019, 719-738. <https://doi.org/10.1016/j.jcde.2018.10.005>
- [24] Pan, Y.; Burnap, A.; Liu, Y.; Lee, H.; Gonzalez, R.; Papalambros, P. Y.: A quantitative model for identifying regions of design visual attraction and application to automobile styling, In *DS 84: Proceedings of the DESIGN 2016 14th International Design Conference*, 2016, 2157-2174.
- [25] Şahin, U.; Şahin, T.: Forecasting the cumulative number of confirmed cases of COVID-19 in Italy, UK and USA using fractional nonlinear grey Bernoulli model, *Chaos, Solitons & Fractals*, 138, 2020, 109948. <https://doi.org/10.1016/j.chaos.2020.109948>
- [26] Salehuddin, R.; Hj. Shamsuddin, S. M.: Hybrid grey relational artificial neural network and auto regressive integrated moving average model for forecasting time-series data, *Applied Artificial Intelligence*, 23(5), 2009, 443-486. <https://doi.org/10.1080/08839510902879384>
- [27] Shahrman, Z. A.; Azlan, O.; Zafruddin, S.; Zaidy, S.; Halim, H.: The challenges of developing styling DNA design methodologies for car design. In *DS 78: Proceedings of the 16th International conference on Engineering and Product Design Education (E&PDE14)*, Design Education and Human Technology Relations, University of Twente, The Netherlands, 04-05.09. 2014, 738-743.
- [28] Shieh, M.-D.; Li, Y.; Yang, C.-C.: Comparison of multi-objective evolutionary algorithms in hybrid Kansei engineering system for product form design, *Advanced Engineering Informatics*, 36, 2018, 31e42. <https://doi.org/10.1016/J.AEI.2018.02.002>.
- [29] Stouffs, R.: Description grammars: Precedents revisited, *Environment & Planning B Urban Analytics & City Science*, 2, 2018, 1-21. <https://doi.org/10.1177/0265813516667301>
- [30] Su, J. N.; Zhao, H. J.; Wang, R. H.; Zhang, S. T.: Product image form optimization design based on support vector machine and particle swarm optimization, *Journal of Machine Design*, 32(1), 2015, 105-109. <https://doi.org/10.13841/j.cnki.jxsj.2015.01.022>
- [31] Sun, X.; Sun, W.; Wang, J.; Zhang, Y.; Gao, Y.: Using a Grey-Markov model optimized by Cuckoo search algorithm to forecast the annual foreign tourist arrivals to China, *Tourism Management*, 52, 2016, 369-379. <https://doi.org/10.1016/j.tourman.2015.07.005>
- [32] Tamiloli, N.; Venkatesan, J.; Ramnath, B. V.: A grey-fuzzy modeling for evaluating surface roughness and material removal rate of coated end milling insert, *Measurement*, 84, 2016, 68-82. <https://doi.org/10.1016/j.measurement.2016.02.008>
- [33] Toh, C. A.; Starkey, E. M.; Tucker, C. S.; Miller, S. R.: Mining for creativity: Determining the creativity of ideas through data mining techniques, In *International Design Engineering Technical Conferences and Computers and Information in Engineering Conference*, 58219, 2017, V007T06A010. <https://doi.org/10.1115/DETC2017-68304>
- [34] Usama, M.; Arif, A.; Haris, F.; Khan, S.; Afaq, S. K.; Rashid, S.: A data-driven interactive system for aerodynamic and user-centered generative vehicle design. In *2021 International Conference on Artificial Intelligence (ICAI)*, 2021, 119-127.

- [35] Wang, L.: Improved NN-GM (1, 1) for postgraduates' employment confidence index forecasting, *Mathematical Problems in Engineering*, 2014. <https://doi.org/10.1155/2014/465208>
- [36] Wang, K., Zhao, Z. Q.; Nie H.: An automobile form design method based on the form evolution, *Modern Manufacturing Engineering*, 07, 2009, 33-36. <https://doi.org/10.16731/j.cnki.1671-3133.2009.07.023>
- [37] Wang, X., Xie, N.; Yang, L.: A flexible grey Fourier model based on integral matching for forecasting seasonal PM2. 5 time series. *Chaos, Solitons & Fractals*, 162, 2022, 112417. <https://doi.org/10.1016/j.chaos.2022.112417>
- [38] Wang, Z. X.: An optimized Nash nonlinear grey Bernoulli model for forecasting the main economic indices of high technology enterprises in China. *Computers & Industrial Engineering*, 64(3), 780-787. <https://doi.org/10.1016/j.cie.2012.12.010>
- [39] Wang, Z. X.; Ye, D. J.: Forecasting Chinese carbon emissions from fossil energy consumption using non-linear grey multivariable models, *Journal of Cleaner Production*, 142, 2017, 600-612. <https://doi.org/10.1016/j.jclepro.2016.08.067>
- [40] Xu, J.; Wang, X. Y.; Huang, P.; Wang, Y.; Chu; Y. T.: Research on prediction methods of automobile styling based on the grey correlation theory, *Journal of Machine Design*, 33(2), 2016, 114-117. <https://doi.org/10.13841/j.cnki.jxsj.2016.02.023>
- [41] Xu, Q. Y.; Yang, M. L.; Liu, W. D.; Liu, C. J.; Yan, H. M.: Product form feature evolution forecasting based on IGMBPM model. *Computer-Aided Design and Applications*, 13(4), 2016, 431-439. <http://dx.doi.org/10.1080/16864360.2015.1131531>
- [42] Yang, W.; Su, J.; Zhang, X.; Qiu, K.; Zhang, S.: Research on Product Primitives Recognition in a Computer-aided Brand Product Development System, *Computer-Aided Design and Applications*, 18(6), 2021, 1146-1166. <https://doi.org/https://doi.org/10.14733/cadaps.2021.1146-1166>
- [43] Zeng D; He M; Tang X; et al.: Cognitive association in interactive evolutionary design process for product styling and application to SUV design, *Electronics*, 9(11): 2020, 1960. <https://doi.org/10.3390/electronics9111960>
- [44] Zhang, S.; Liu, S.; Su, J.; Zhou, A.; Wang, S.: An evolutionary design method of product form inspired by spider-webs, *Computer-Aided Design and Applications*, 2022. DOI: <https://doi.org/10.14733/cadaps.2022.1-25>
- [45] Zhang, W. Q., Zhao J. H.; Tan H.: Research on the Formation of Audi Brand and Design Feature, *Decoration*, 07, 2011, 75-77. <https://doi.org/10.16272/j.cnki.cn11-1392/j.2011.07.011>

Appendix A:

<i>Coordinate</i>	<i>Data Sequence</i>
X_1	{-110.45, -55.50, -23.20, -16.44, -28.11, -35.48, -24.75, -44.77, -26.90}
X_2	-116.06, -63.95, -23.84, -16.06, -27.75, -34.31, -25.54, -42.84, -30.00
X_3	-116.06, -63.28, -22.67, -15.66, -24.73, -27.78, -22.57, -34.90, -27.58
X_4	-110.45, -59.50, -20.15, -11.97, -19.43, -16.37, -15.82, -21.91, -17.45
X_5	-110.45, -59.50, -18.40, -10.51, -18.41, -14.62, -12.48, -21.91, -10.95
X_6	-110.45, -59.50, -13.65, -6.48, -16.35, -11.87, -8.48, -21.91, 1.64
X_7	-110.45, -59.50, -8.28, -1.96, -14.23, -9.04, -3.81, -21.91, 20.33
X_8	-58.10, -50.43, 41.02, 43.56, 22.08, 39.54, 12.75, -13.46, 24.51

<i>Coordinate</i>	<i>Data Sequence</i>
X_9	-5.76, 43.40, 104.69, 89.07, 58.40, 76.07, 61.49, 18.53, 36.54
X_{10}	46.59, 84.66, 138.67, 134.59, 94.75, 101.72, 86.19, 72.78, 52.11
X_{11}	53.49, 84.66, 144.29, 138.40, 106.20, 103.35, 86.19, 72.78, 66.10
X_{12}	59.73, 84.66, 149.24, 141.56, 116.63, 101.34, 86.19, 72.78, 80.08
X_{13}	63.44, 84.66, 152.31, 143.54, 124.16, 98.19, 86.19, 72.78, 91.09
X_{14}	64.12, 93.20, 156.72, 146.46, 131.45, 60.26, 92.94, 81.54, 106.26
X_{15}	63.24, 101.06, 160.50, 148.81, 138.15, 22.33, 98.68, 92.56, 116.66
X_{16}	60.21, 97.17, 163.66, 150.57, 144.75, -16.09, 102.17, 105.83, 123.81
X_{17}	58.57, 97.17, 164.43, 151.58, 146.36, -16.09, 103.09, 105.83, 123.81
X_{18}	51.47, 97.17, 162.91, 149.31, 144.92, -16.09, 99.71, 105.83, 123.81
X_{19}	43.48, 97.17, 160.71, 146.12, 142.29, -16.09, 95.55, 105.83, 123.81
X_{20}	-11.39, -51.74, 102.32, 94.40, 86.76, -22.56, 55.04, 48.40, 48.37
X_{21}	-80.02, 6.32, 43.98, 42.68, 33.42, -29.02, 15.63, -35.90, -2.84
X_{22}	-110.45, -55.50, -12.34, -9.04, -17.78, -35.48, -24.75, -44.77, -23.94
X_{23}	-110.45, -55.50, -18.07, -13.23, -23.85, -35.48, -24.75, -44.77, -24.76
X_{24}	-110.45, -55.50, -22.82, -16.58, -28.27, -35.48, -24.75, -44.77, -25.75
X_{25}	-110.45, -55.50, -23.20, -16.44, -28.11, -35.48, -24.75, -44.77, -26.90
Y_1	163.32, 154.10, 234.83, 230.99, 209.34, 244.41, 230.11, 248.23, 240.46
Y_2	186.99, 164.37, 244.22, 243.02, 222.72, 272.32, 249.87, 278.44, 268.07
Y_3	207.07, 170.21, 252.57, 255.73, 236.31, 293.20, 268.11, 299.86, 285.89
Y_4	232.65, 184.47, 259.88, 266.56, 245.99, 307.85, 285.25, 312.03, 297.58
Y_5	232.65, 184.47, 264.96, 270.84, 247.87, 310.09, 288.70, 312.03, 292.78
Y_6	232.65, 184.47, 268.46, 273.71, 248.71, 311.11, 293.62, 312.03, 282.20
Y_7	229.21, 183.46, 269.08, 273.67, 244.72, 307.62, 280.58, 299.79, 277.94
Y_8	229.21, 183.46, 269.08, 273.67, 244.72, 307.62, 280.58, 299.79, 277.94
Y_9	228.27, 183.46, 266.94, 272.75, 239.38, 284.34, 264.95, 287.36, 274.75
Y_{10}	225.84, 183.46, 261.00, 253.64, 233.86, 241.65, 259.54, 276.36, 271.11
Y_{11}	220.78, 183.46, 260.02, 252.04, 232.12, 238.95, 259.54, 276.36, 268.11
Y_{12}	215.88, 183.46, 256.72, 249.19, 226.33, 235.53, 259.54, 276.36, 264.43
Y_{13}	212.03, 183.46, 251.91, 245.56, 217.54, 235.63, 259.54, 276.36, 261.07

<i>Coordinate</i>	<i>Data Sequence</i>
Y_{14}	195.00, 172.09, 245.00, 240.21, 209.01, 236.84, 246.30, 255.44, 245.03
Y_{15}	175.98, 162.95, 237.34, 234.86, 200.48, 238.45, 230.26, 235.67, 229.93
Y_{16}	161.46, 152.28, 228.93, 229.51, 191.95, 241.28, 214.81, 216.66, 215.64
Y_{17}	153.63, 152.28, 226.87, 226.48, 189.87, 241.28, 210.72, 216.66, 215.64
Y_{18}	148.14, 152.28, 224.68, 223.35, 186.84, 241.28, 206.95, 216.66, 215.64
Y_{19}	148.54, 152.28, 224.68, 223.35, 186.78, 241.28, 207.41, 216.66, 215.64
Y_{20}	151.24, 152.24, 224.68, 223.35, 185.53, 241.78, 211.96, 218.08, 225.98
Y_{21}	157.83, 152.20, 224.68, 223.35, 189.09, 242.88, 218.03, 232.48, 232.96
Y_{22}	163.32, 154.10, 224.68, 223.35, 196.97, 244.41, 230.11, 248.23, 242.88
Y_{23}	163.32, 154.10, 224.68, 223.35, 197.91, 244.41, 230.11, 248.23, 241.98
Y_{24}	163.32, 154.10, 229.12, 226.81, 203.21, 244.41, 230.11, 248.23, 241.13
Y_{25}	163.32, 154.10, 234.83, 230.99, 209.34, 244.41, 230.11, 248.23, 240.46